Auton Robot (2007) 22:305–319
DOI 10.1007/s10514-006-9722-z

Human-robot cooperation control for installing heavy construction materials

Seung Yeol Lee · Kye Young Lee · Sang Heon Lee · Jin Woo Kim · Chang Soo Han

Received: 22 May 2006 / Revised: 22 May 2006 / Accepted: 10 July 2006 / Published online: 13 September 2006

Abstract Previously, ASCI (Automation System for Curtain-wall Installation) which combined with a multi-DOF manipulator to a mini-excavator was developed and applied on construction site. As result, the operation by one operator and more intuitive operation method are proposed to improve ASCI's operation method which need one person with a remote joystick and another operating an excavator. The human-robot cooperative system can cope with various and untypical constructing environment through the real-time interacting with a human, robot and constructing environment simultaneously. The physical power of a robot system helps a human to handle heavy construction materials with relatively scaled-down load. Also, a human can feel and response the force reflected from robot end effecter acting with working environment. This paper presents the feasibility study regarding the application of the proposed human-robot cooperation control for construction robot through experiments on a 2DOF manipulator.

Keywords Construction robot · Impedance control · Human-robot cooperation · Force assist ratio · Force reflection

S. Y. Lee (✉) · C. S. Han (✉)
Department of Mechanical Engineering, Hanyang University,
17, Haengdang-dong, Seongdong-gu, Seoul, Korea, 133-791
e-mail: e-mail: suprasy@paran.com
e-mail: cshan@hanyang.ac.kr

K. Y. Lee · S. H. Lee
SAMSUNG CONSTRUCTION,
4th Fl., Seohyun Bldg. 270-2, Seohyun-Dong, Bundang-Gu,
Sungnam-Si, Gyonggi-Do, Korea, 463-771

K. Y. Lee
e-mail: kyle@samsung.com

S. H. Lee
e-mail: shlee31@samsung.com

J. W. Kim
Department of Mechatronics Engineering, Hanyang University,
Sa 1 dong, Sangrok gu, Ansan, Kyonggi Do,
South Korea, 426-791
e-mail: gasigogi7@orgio.net

1 Introduction

The issue of applying "Automation System and Robotics in Construction" has been raised as a result of the need for improvement in the safety, productivity, quality and working environment (Roozbeh, 1985; Warszawski, 1985). The first construction robot, which appeared in Japan in 1983, was designed as a manipulator to spray fireproofing material on steel. Since then, many robots have been applied for different purposes. Gambao et al. obtained the robotic systems that improve the manual block assembly tasks reducing dramatically the construction time and efforts (Gambao et al., 2000). Choi et al. presented a construction robot that is a hybrid-type using pneumatic actuator and servo motor (Choi et al., 2005). The hybrid-type robot can be used in a window glass mounting or panel fixing. Ostoja-Starzewski and Skibniewski designed the master-slave force-feedback hydraulic manipulator that contributes to the flexibility and productivity enhancement of related work tasks (Ostoja-Starzewski and Skibniewski, 1989). Santos et al. introduced a manipulator to assist the operators in handling and installing pre-manufactured plaster for indoor-wall construction (Santos et al., 2003). Skibniewski and Wooldridge described an automated materials handling system concept for managing and handling construction materials within automated building construction systems (Skibniewski and Wooldridge, 1992). Masatoshi et al. proposed the automated building interior finishing system, and a

Fig. 1 Workers & curtain wall

suitable structural work method is also described (Masatoshi et al., 1996). Isao et al. discussed the appropriateness of automation technology for installation of curtain wall (Isao et al., 1996).

Recently, the trend in architectural forms has been towards larger and taller buildings. As the tendency changes towards larger and taller buildings and structure, it has been accompanied by advances in the study and development of new building materials. Exterior curtain walls, which are responsible for adiabatic function, water-tightness and the aesthetics of a building, are of particular interest to the building construction field.

But, the process is complicated and hazardous, relying on unsuited equipment and a large amount of manpower like Fig. 1.

In order to solve these problems, an automation system combining a commercial mini-excavator and a multi-DOF manipulator was proposed in Fig. 2.

Although this method improved working conditions at construction sites more or less, it still left difficulties in precision construction and operation of equipments as the equipment, which had not been designed for curtain wall installation, were applied. As shown in Fig. 3, therefore, we developed an automation system (ASCI; Automation System for Curtain Wall Installation), suitable for the mechanized construction, which enabled simpler and more precise installation than the existing construction methods did, and, most of all, improved safety during installation works (Lee, 2006).

Through the case studies on constructions, to which ASCI was applied, however, we could find some factors

Fig. 2 A mini-excavator with attachment

Fig. 3 ASCI (Automation System for Curtain wall Installation)

to be improved. Unlike the automation lines of the general manufacturing industry, construction sites rarely shows repeated operational patterns use to its unstructured processes. Thus, we deduced the following improvements.

- A robot that can follow operator intention in various works at unstructured construction sites
- A robot that shares work space with an operator
- Coordination of operator's force and the robot's amplified force
- Intuitive operational method that can reflect dexterity of an operator

One of the solutions for these requirements is the technology of human-robot cooperation (Fujisawa et al., 1991a, 1991b, 1991c). Studies on the human-robot cooperation have been ceaselessly performed so far. In 1960s, the Department of Defense developed the 'Suit of Armor', which enhanced the capability of soldiers in carrying heavy materials (Miller, 1968). In 1962, the Cornell Aeronautical Lab. conducted a study on the 'Master-Slave System', which allowed a man to walk with heavy materials (Miller, 1968). The study on the Master-Slave System led up to the 'Hardiman' of GE that existed from 1966 to 1971 (Mosher, 1967). Afterward, Kazerooni suggested the 'Extender' that, unlike the Master-Slave System, delivered the operational force and information to a robot at the same time by the contact force (Kazerooni, 1989, 1991). The Extender presented unique features of modeling through using each impedance of the three factors: human arm, extender and environment, and the controller for the operator's force and robot's force. Kosuge suggested a control algorithm for the man-robot cooperation, using maneuverability and amplification factor (Kosuge, 1993). To implement the human-robot cooperation in restricted environments, the impedance control method, which was proposed by Hogan, has been used as a basic force control method (Hogan, 1985).

In this paper, we introduce a robot control method, as shown in Fig. 4, for installation of heavy construction materials in cooperation between an operator and a robot. Especially, considerations on interactions among the operational force, robot and environment are applied to design of the robot controller. That is to say, the system, to which the introduced control method is applied, allows an operator to handle heavy materials as if he did it by himself or herself, by exerting operational force with a certain power assist ratio. Also, this system enables an operator to perform operations more intuitively by allowing him or her to feel reaction forces from environments during an operation.

The contents of the study, to implement the proposed control method, include the followings. First of all, we modeled the interactions among the human, robot and environment, using the target dynamics. We designed an impedance controller for the human-robot cooperation, considering each environment-contacting case and non-environment-contacting case, based on the human-robot-environment modeling. In case a heavy material does not contact the environment (an unconstrained condition), a motion controller was mounted inside the impedance controller to improve the position following performance. Finally, we examined the influences, which the parameters of the impedance model gave to performance of the cooperation system, through a 2DOF experimental system.

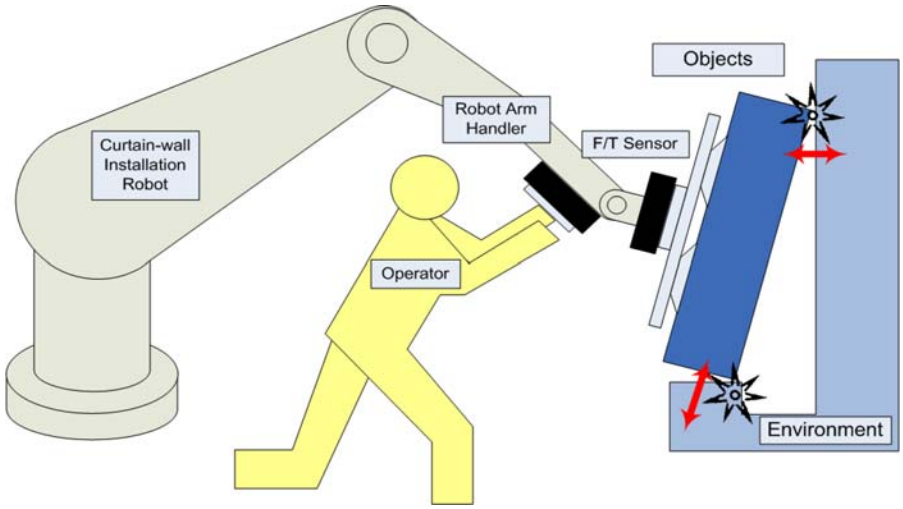

Fig. 4 Concept of human-robot cooperation

a) Unconstrained condition

b) Constrained condition

Fig. 5 Heavy material handling with HRC

2 Modeling of human-robot cooperation system

Heavy materials handling operations can be divided into the environment-contacting cases and non-environment-contacting cases as shown in Fig. 5. During contact with an environment, it acts as a dynamic constraint and affects an operator. These constraining conditions are usually avoidable through controlling actions, but some of phenomena can be considered as the 'virtual dynamic behaviors" against external forces from the environments including the operator. The mechanical relationship, between an external force and the motion toward the external force, is defined as the impedance, and a desired target is defined as the target dynamics.

The operational force is measured by the operational force sensor that is mounted on the last link of a manipulator, and the contact force from an environment is measured by the experimental force sensor that is located between the last link and the end effector.

While the case, an operator handles a heavy material on an obstacle-free place, is defined as the unconstrained condition, the case, an operator performs work under interactions with environments, is defined as the operation in the constrained condition.

2.1 Unconstrained condition

The case, in which an operator handles heavy materials on an obstacle-free place, is defined as the operation in unconstrained conditions. In Fig. 6, the force (torque), measured by the operational force sensor which is generated by the interaction between the operator and a heavy material, is $F_h(T_h)$, and the impedance parameters, that are related to a desired dynamic behavior, are $M_{pt}(M_{ot})$ and $B_{pt}(B_{ot})$ ($n \times n$ positive definite diagonal inertia and damping matrices) respectively. Here, the desired dynamic behavior of a robot can be given, with the input F_h, (T_h), by an impedance Eq. (1). The subscript "p" stands for the position and "o" stands

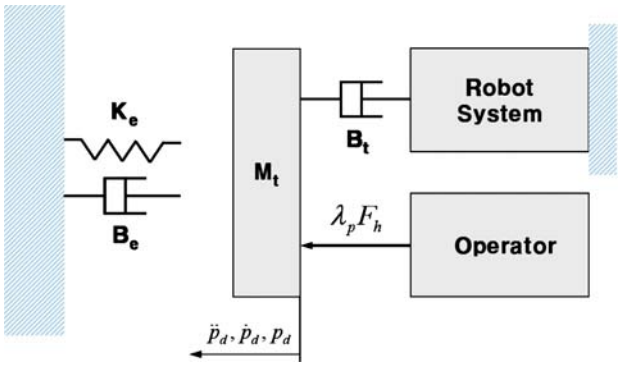

Fig. 6 Unconstrained condition

for the orientation, and λ means the power assist ratio of an operator.

$$
\begin{aligned}
&M_{pt}\ddot{p}_d + B_{pt}\dot{p}_d = \lambda_p F_h \\
&M_{ot}\ddot{\varphi}_d + B_{ot}\dot{\varphi}_d = \lambda_o T^T(\varphi_d) T_h \\
&\text{where,} \quad \varphi = [\,\alpha\ \beta\ \gamma\,]^T \\
&\qquad T = \begin{bmatrix} 0 & -s\alpha & c\alpha s\beta \\ 0 & c\alpha & s\alpha s\beta \\ 1 & 0 & c\beta \end{bmatrix}
\end{aligned} \tag{1}
$$

The K (Stiffness Matrices) parameter, having the property of a spring, was excluded as it disturbed the operation to move a heavy material to a desired position with the operational force. Ultimately, adjusting each of the impedance parameters equals to adjusting the dynamic behavior of a virtual system. The dynamic behavior, generated from the impedance Eq. (1) when an operator applies force to a virtual system, is used as a reference that a robot system should follow to move a heavy material. Table 1 shows the inputs and outputs for the modeling of an operator and an environment from the viewpoint of a robot in an unconstrained condition. Upon input of the operational force, the robot system outputs a desired dynamic behavior.

2.2 Constrained condition

In Fig. 7, the force (torque) that was measured by the operational force sensor is $F_h(T_h)$, and the force (torque) that was measured by the experimental force sensor is $F_e(T_e)$. With the input values of $F_h(T_h)$ and $F_e(T_e)$, unlike an operation in the unconstrained condition, the desired dynamic behavior of a robot can be described by an impedance Eq. (2). For the same reason with case of the unconstrained condition, the

Table 1 Input & output in the unconstrained condition

	Operator	Environment
Input	$F_h(T_h)$	–
Output	$\ddot{p}_d,\ \dot{p}_d,\ p_d(\ddot{\varphi}_d, \dot{\varphi}_d, \varphi_d)$	–

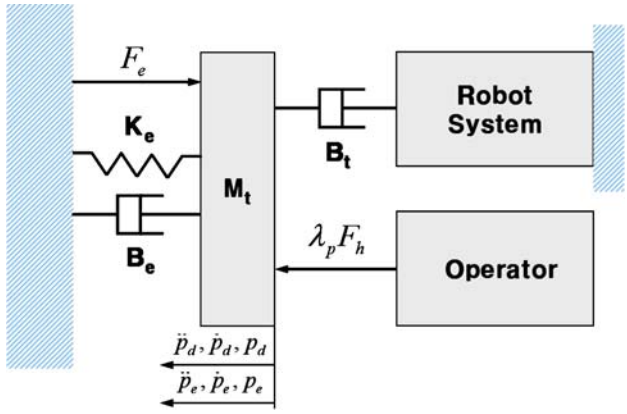

Fig. 7 Constrained condition

K (Stiffness Matrices), having the property of a spring, was excluded.

$$
\begin{aligned}
&M_{pt}\ddot{p}_d + B_{pt}\dot{p}_d = \lambda_p F_h - F_e \\
&M_{ot}\ddot{\varphi}_d + B_{ot}\dot{\varphi}_d = T^T(\varphi_d)(\lambda_o T_h - T_e)
\end{aligned} \tag{2}
$$

In case interactions with an environment occur (a constraint condition), the end effector should endow with a behavior, considering the compliance. In this regard, we defined the relationship between the contact force (torque) and the position error of the end effector, through the generalized active impedance, as in (3). Thus, the end effector can have linear and dependant impedance characteristics to the translation part, for which the contact force F_e was considered, and the rotation part, for which the equivalent contact moment $T^T T_e$ was considered. In the (3), $M_{pe}(M_{oe})$, $B_{pe}(B_{oe})$, $K_{pe}(K_{oe})$ are the impedance parameters that determine a dynamic behavior of the end effector for interactions with an environment.

$$
\begin{aligned}
&M_{pe}\Delta\ddot{p}_{de} + B_{pe}\Delta\dot{p}_{de} + K_{pe}\Delta p_{de} = F_e \\
&M_{oe}\Delta\ddot{\varphi}_{de} + B_{oe}\Delta\dot{\varphi}_{de} + K_{oe}\Delta\varphi_{de} = T^T(\varphi_e)T_e \\
&\text{where, } \Delta p_{de} = p_d - p_e
\end{aligned} \tag{3}
$$

Table 2 shows the inputs and outputs for of an operator and an environment from the viewpoint of a robot in a constraint condition. Upon input of the operational force and environmental contact force to a robot, the robot system outputs a desired dynamic behavior. The dynamic behavior is determined, as shown in (3), by the environmental contact force and impedance characteristics. The position error indicates the difference between the desired dynamic behavior and the actual dynamic behavior of the end effector. That is to say, it explains that a robot system cannot practically

Table 2 Input & output in the constrained condition

	Operator	Environment
Input	$F_h(T_h)$	$F_e(T_e)$
Output	$\ddot{p}_d,\ \dot{p}_d,\ p_d(\ddot{\varphi}_d, \dot{\varphi}_d, \varphi_d)$	$\Delta\ddot{p}_{de}, \Delta\dot{p}_{de}, \Delta p_{de}$ $(\Delta\ddot{\varphi}_{de}, \Delta\dot{\varphi}_{de}, \Delta\varphi_{de})$

follow a desired dynamic behavior, but indicates a level of compliance with an environment.

3 Control strategy of human-robot cooperation work

3.1 Adjustment of impedance parameters

Previously in Fig. 5, we categorized the heavy-materials handling operation through the human-robot cooperation-work into the environment-contacting case and the non-environment-contacting case. From the viewpoint of operational characteristics, the former case can be thought as the press fit operation under interactions with already-installed curtain walls, which requires relatively higher stability. On the contrary, the latter case can be considered as the operation of moving curtain walls promptly to an installation site, which requires relatively higher mobility. In a human-robot cooperative system, we can make an object have impedance characteristics through the use of robot. To get the high stability, the object may have a damping characteristic. However, too much damping decreases the mobility of the system. In this strategy, the impedance parameters of the robot's end-effector are adjusted corresponding to the process of the work of a human operator. Figure 8 shows the proposed control strategy for adjusting of impedance parameters.

In the impedance (2), the impedance parameters $M_{pt}(M_{ot})$ and $B_{pt}(B_{ot})$ are switched to proper values when an operator requires stability or mobility according to the work process. The appropriate parameter values are determined through enough simulations with an experimental system. Also, each of the impedance parameters should be adjusted by stage according to the choice of an operator. This adjusting way is also applied exactly to adjustment of the power assist ratio (λ) of an operator.

3.2 Inner motion control

The selection of good impedance parameters that guarantee a satisfactory compliant behavior during the interaction may turn out to be inadequate to ensure accurate tracking of the desired position and orientation trajectory when the end effector moves in unconstraint condition. A solution to this drawback can be devised by separating the motion control action from the impedance control action as follows. The motion control action is purposefully made stiffness so as enhance disturbance rejection but, rather than ensuring tracking of a reference position and orientation, it shall ensure tracking of a reference position and orientation resulting from the impedance control action. In other words, the desired position and orientation together with the measured contact force and moment are input to the impedance equation which, via a suitable integration, generates the position and orientation to be used as a reference for the motion control action.

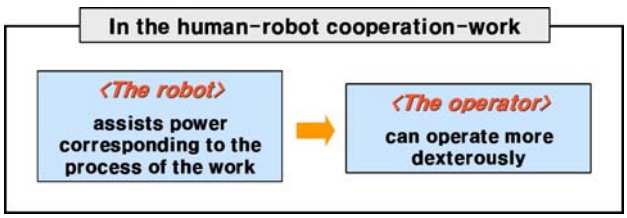

Fig. 8 Target of control strategy

In order to realize the above solution, it is worth introducing a reference frame other than the desired frame specified by a desired position vector p_d and a desired rotation matrix R_d. This frame is referred to as the compliant frame, and is specified by a position vector p_c and a rotation matrix R_c. In this way, the inverse dynamics motion control strategy can be still adopted as long as the actual end effector position p_e and orientation R_e is taken to coincide with p_c and R_c in lieu of p_d and R_d, respectively. Accordingly, the actual end-effector linear velocity $\dot{p}_e$ and angular velocity ω_e are taken to coincide with $\dot{p}_c$ and ω_c, respectively.

A block diagram of the resulting scheme is sketched in Fig. 9 and reveals the presence of an inner motion control loop with respect to the outer impedance control loop.

In view (2), the impedance equation is chosen so as to enforce an equivalent mass-damper-spring behavior for the position displacement when the end effector exerts a force (torque) $F_e(T_e)$ on the environment, i.e.

$$\begin{aligned} &M_{pe}\Delta\ddot{p}_{dc} + B_{pe}\Delta\dot{p}_{dc} + K_{pe}\Delta p_{dc} = F_e \\ &M_{oe}\Delta\ddot{\varphi}_{dc} + B_{oe}\Delta\dot{\varphi}_{dc} + K_{oe}\Delta\varphi_{dc} = T^T(\varphi_e)T_e \\ &\text{where,} \quad \Delta p_{dc} = p_d - p_c \end{aligned} \tag{4}$$

With reference to the scheme in Fig. 9, the impedance control generates the reference position for the inner motion control. Therefore, in order to allow the implementation of the complete control scheme, the acceleration shall be designed to track the position and the velocity of the compliant frame, i.e.

$$\begin{aligned} &a_p = \ddot{p}_c + K_{Dp}\Delta\dot{p}_{ce} + K_{Pp}\Delta p_{ce} \\ &a_o = T(\varphi_e)(\ddot{\varphi}_{ce} + K_{Do}\Delta\dot{\varphi}_{ce} + K_{Po}\Delta\varphi_{ce}) + \dot{T}(\varphi_e, \dot{\varphi}_e)\dot{\varphi}_e \\ &\text{where, } \Delta p_{ce} = p_c - p_e \end{aligned} \tag{5}$$

Notice that p_c and its associated derivatives can be computed by forward integration of the impedance Eq. (4) with input $F_e(T_e)$ available from the force/torque sensor.

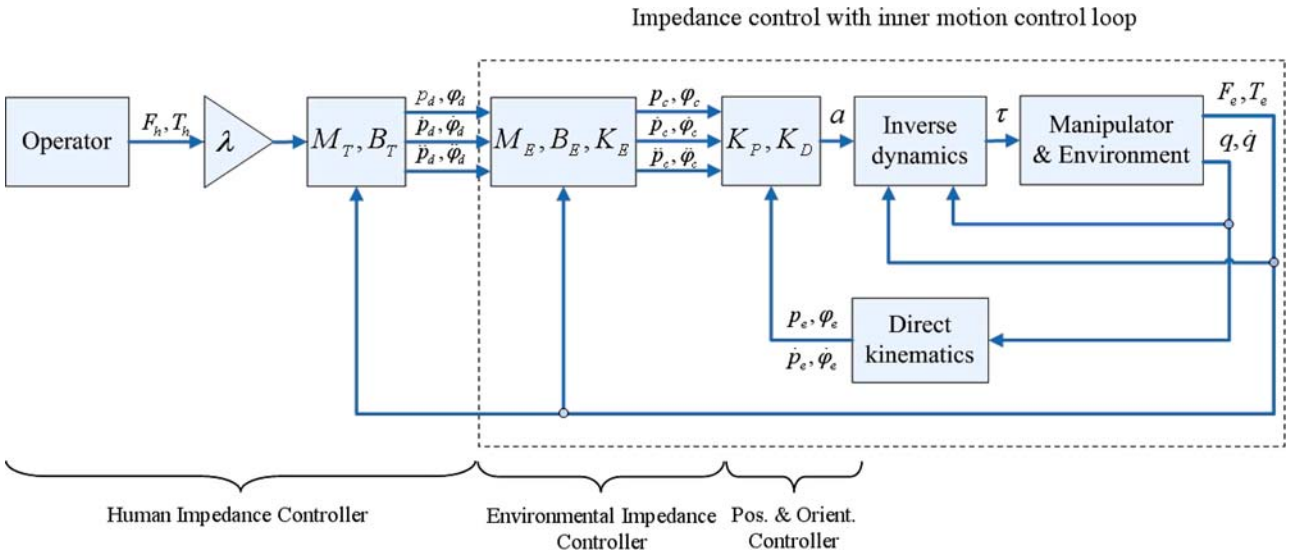

Fig. 9 Control system for human-robot cooperation-work

4 Experimental system

As shown in Figs. 10 and 11, we mounted two sensors in the 2DOF manipulator, moving in the x and y directions. One receives operational signals from an operator, and the other, positioned between the end effector and the 15 kg weighing object, can detect the contact force from the environment. With the signals that are received by the two sensors, the control signals, the manipulator should follow, are generated.

Figure 12 shows a flow chart of the control system. The analog output data of the force/torque sensor is sent to an A/D unit and it provides the force (torque) value to DSP (dspace Co.ltd). The DSP is used for the force analysis and the impedance control of the manipulator. PC/AT (and display) is used for indicating information containing a real time dynamic behavior of the experimental system. DSP and PC/AT are connected by a local network using LAN cable. DSP sends control information to the PC/AT on real time.

The manipulator is controlled using a impedance control with inner motion loop method based on the force control. It assumes that the manipulator follows a commanded force derived by Eq. (6). The sampling time for the force analysis and controlling the manipulator is settled as 1 msec.

$$\begin{bmatrix} F_1 \\ F_2 \end{bmatrix} = \begin{bmatrix} m_1+m_2 & 0 \\ 0 & m_2 \end{bmatrix} \begin{bmatrix} \ddot{d}_1 \\ \ddot{d}_2 \end{bmatrix} + \begin{bmatrix} m_1 g + m_2 g \\ 0 \end{bmatrix} + \begin{bmatrix} F_{ey} \\ F_{ez} \end{bmatrix} \tag{6}$$

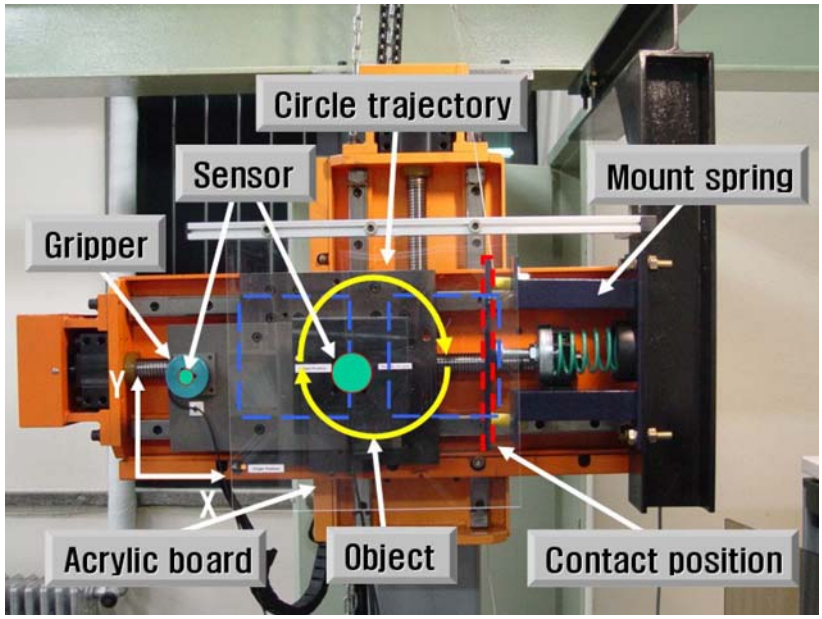

Fig. 10 Configuration of experimental system

Fig. 11 2DOF manipulator

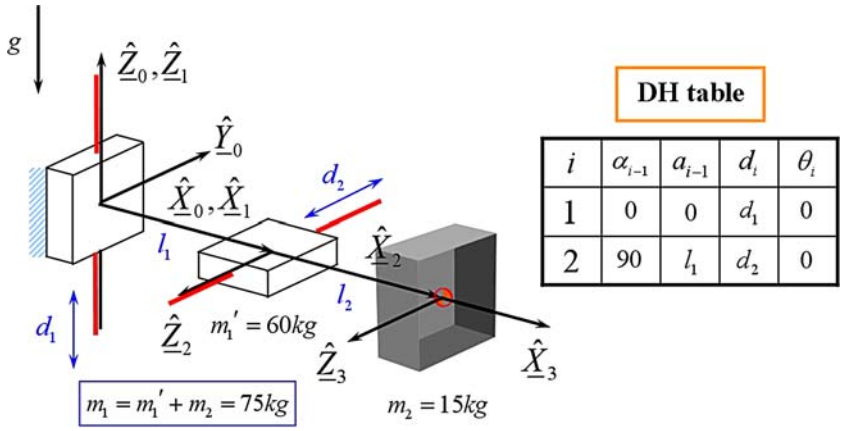

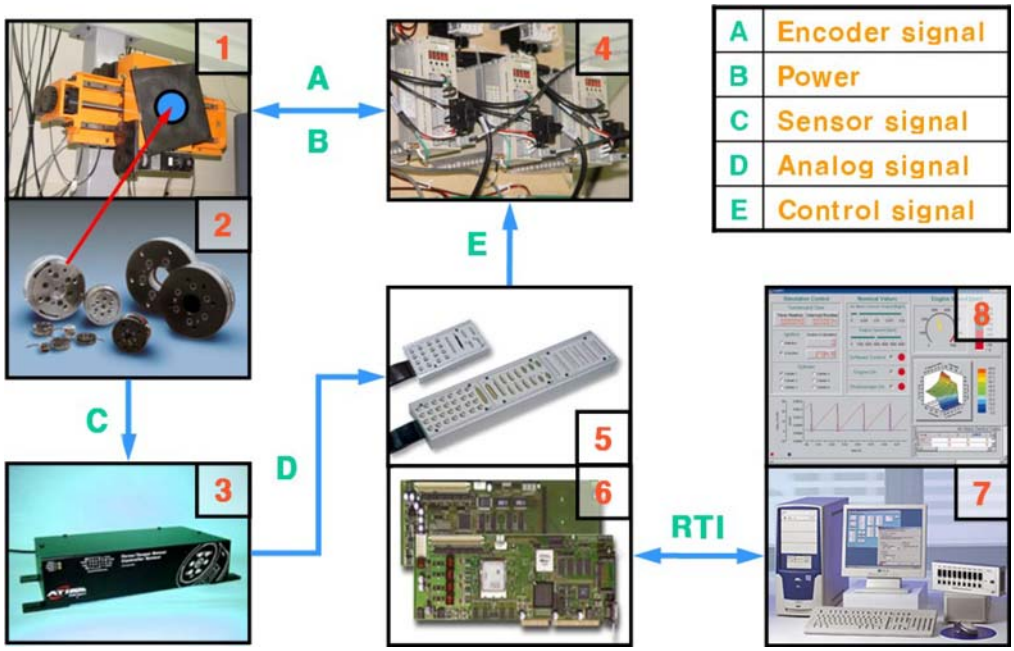

Fig. 12 Flow chart of control system

A mount string was used for the environmental system. The stiffness for an actual environment can be adjusted through replacement of the spring.

5 Experiment and results

Figure 13 shows a coordinate system of experimental system. The experimental methods for the human-robot cooperation-work can be categorized into four staged.

① An indicator, mounted on an object, automatically moves to the home position from the original position.
② The operator applies force to the gripper, so that the indicator follows a circle trajectory that is described on an acrylic board.
③ Based on the operational force, the robot follows the circle trajectory through the impedance control in the unconstraint condition.
④ The robot contacts a mount spring (environmental system) while following the circle trajectory. The contact force, generated at this time, enables the impedance control, and the robot finishes a heavy material handling operation in compliance with an environment.

The robot is to follow a circle trajectory, having a diameter of 0.2 m, in almost 180 sec. This experiment did not require a strict tracking work with respect to the indicated trajectory. Because we should respect his intention or the working condition for the human-robot cooperation. It is expected that a profile of applied force and position of the end effector are observed as a smooth curved line without any disturbance. Experiments are conducted after some practices by a healthy man aged 29 years.

The experimental contents are as follows: Firstly, the influences of each parameter are to be observed for adjustment of the impedance parameters. Secondly, the performance of

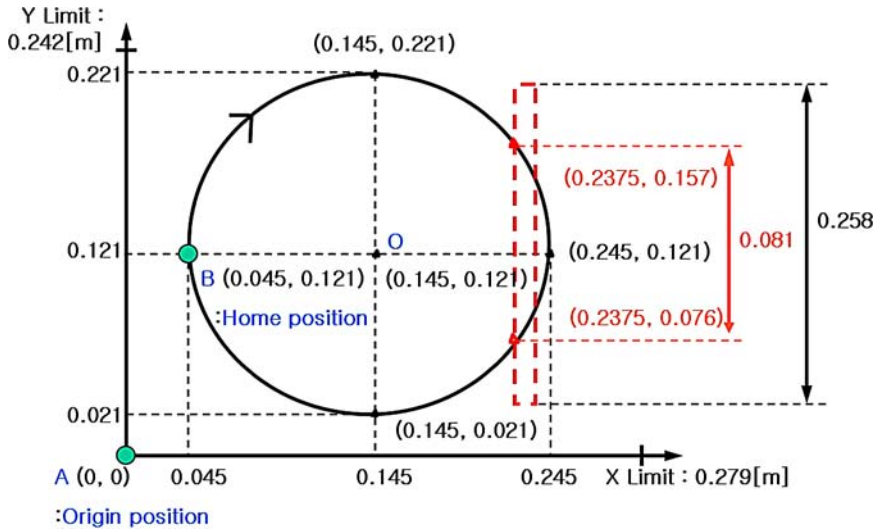

Fig. 13 A coordinate system of experimental system

the suggested impedance control with inner motion control loop is to be evaluated to reduce the position following error for operation of a robot in an unconstrained condition. Thirdly, the influences of F_h and F_e, according to change of the power assist ratio (λ) of an operator, are to be studied. Finally, the changes of F_h and F_e, according to the changes of the actual environmental stiffness, are to be investigated.

5.1 Influence of impedance parameters

To meet the purpose of this experiment, we performed the experiment through DOE (Design of Experiment). The factors are given as the impedance parameters M_{pt} (M_{ot}) and B_{pt} (B_{ot}) in (2), and the levels are given as 1, 3, and 10. The characteristic values according to results of the experiment are described in Figs. 14 and 15. The force, used for the two experiments, is 5 N and applied for around 10 sec. The K value is to be set to 1 N/m for convergence of graphs. Figure 14 shows a case, where the factor is M_{pt}, which is related to an operation that requires mobility in heavy-materials-handling operational process. That is to say, this operation does not require relatively higher stability, but requires prompt movement of an object to a desired position with small operational force. As the M_{pt} value rises, an object can be moved to a long-distance place with small operational force. However, it tends to reduce the stability as shown in the Fig. 14.

Figure 15 shows a case, where the factor is B_{pt}, which is related to an operation that requires stability in heavy-materials-handling operational process. That is to say, this case does not require relatively higher mobility, but requires a precise and stable operation. As B_{pt} (B_{ot}) value rises, the distance of movement by the same operational force gets shorter. As the mobility is reduced, the more demanding

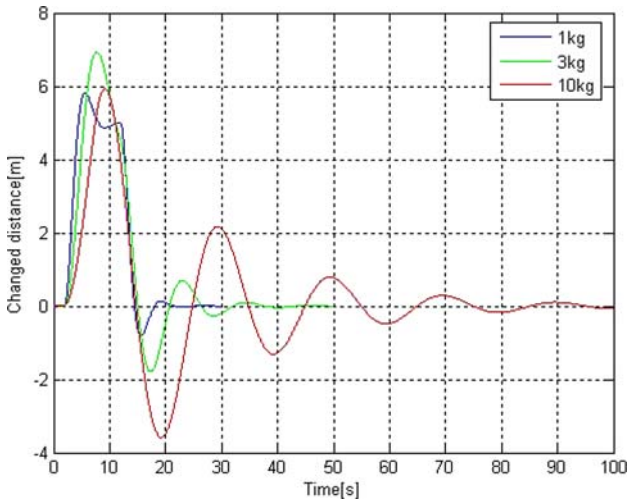

Fig. 14 Influence of impedance parameter $M_{pt}(M_{ot})$

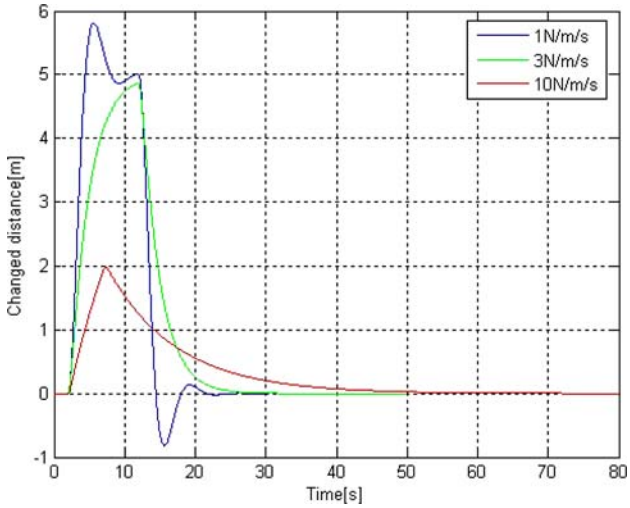

Fig. 15 Influence of impedance parameter $B_{pt}(B_{ot})$

force may make an operator feel the minimum moving distance shorter.

The two factors are related to mobility and stability, and interact with each other. Therefore, these two factors should be traded off appropriately so that a robot system can have the maximum mobility in the range of securing the system stability or vice versa. Also, stage-by-stage adjustment of each factor should be available in consideration of an operator's choice. The M_{pt} and B_{pt} values, used in the experiments, were 50I and 2500I respectively for the mobility-requiring operation (unconstraint condition), and 15I and 7500I respectively for the stability-requiring operation (constraint condition).

5.2 Influence of inner motion control loop

Figure 16 shows a graph that was achieved by applying changes of the environmental stiffness factor (K_{pe}) to the proposed impedance control system. Without the operational force, the constant force, which is input to the controller, makes the robot follow an already-programmed circle trajectory (desired). As shown in the graph, it can be recognized that the path tracking accuracy is rather poor during execution of the whole tasks if the stiffness parameter is small. The small stiffness parameter also causes reduction of the contact force in the constraint condition. These results occur due to a larger end effector position error in operation.

To solve these problems, we proposed the impedance control with an inner motion control loop in this paper. The inner motion loop gains in (5) have been set as $K_{Dp} = 1.5\mathrm{I}$ and $K_{Pp} = 15\mathrm{I}$. Figure 17 shows a graph that compares a case with the inner motion control loop and a case without the inner motion control loop when the external environmental stiffness factor is 1000 N/m. As indicated in the graph, the robot operation without the inner motion control loop shows inferior desired-position-following performance in an unconstraint condition. By using the inner motion control loop, the high following performance can be obtained as shown in the Fig. 17.

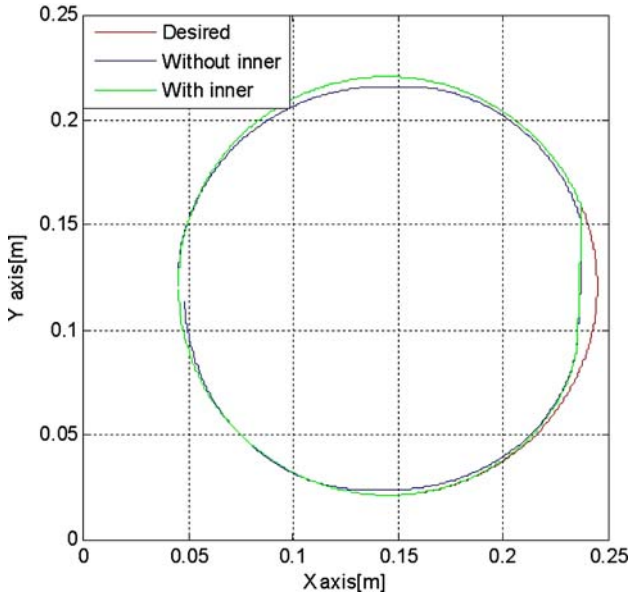

Fig. 17 With inner motion control loop

5.3 Influence of power assist ratio

Figure 18 shows a result graph that was obtained from the suggested experimental method for human-robot cooperation-work. The operator applies force to the gripper

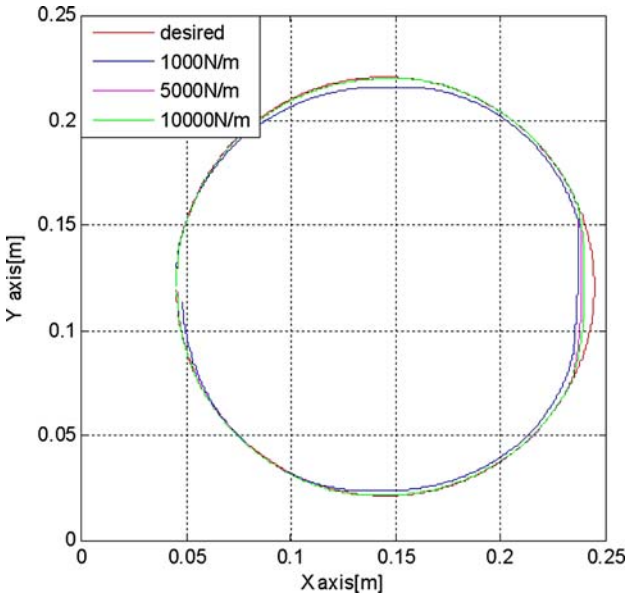

Fig. 16 Without inner motion control loop

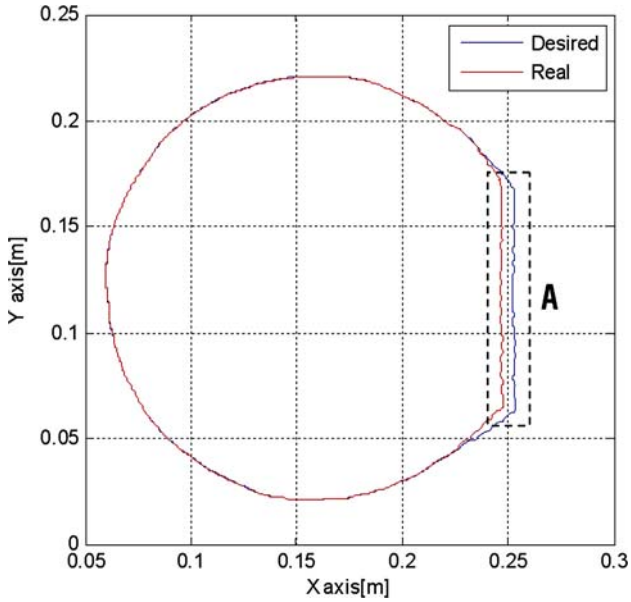

Fig. 18 Experiment result

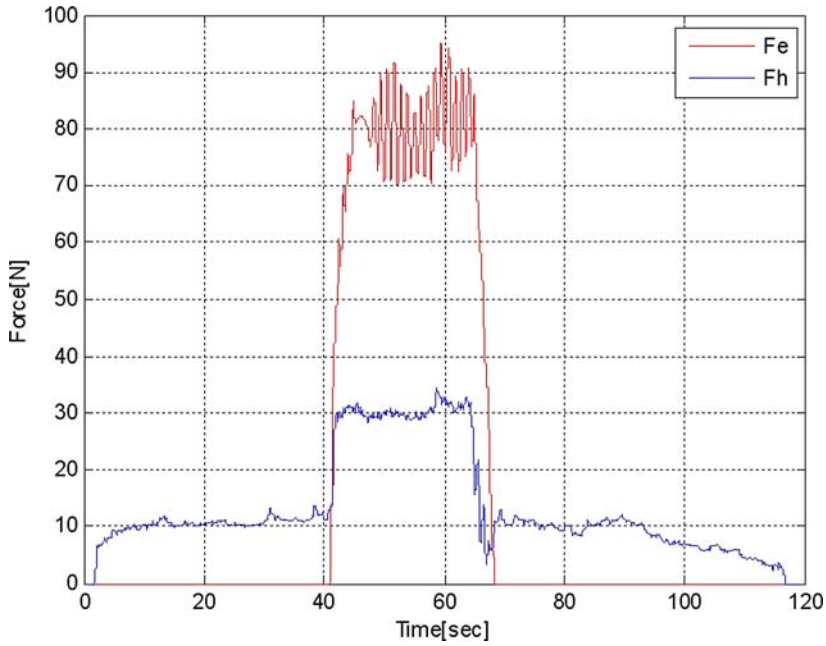

Fig. 19 F_e, F_h at $K_{pe} = 8000\text{I}$ and $\lambda = 3$

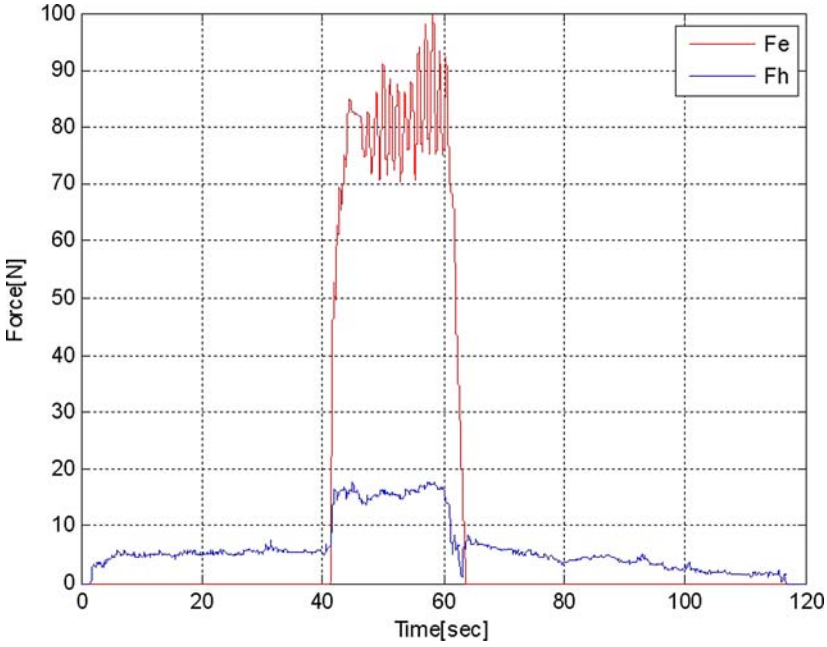

Fig. 20 F_e, F_h at $K_{pe} = 8000\text{I}$ and $\lambda = 6$

so that the indicator, mounted in the object, can follow the circle trajectory that is described on the acrylic board. In the graph, the part A is the area where the object contacts the environment (mount spring). The compliance, determined by the impedance parameters of the environment, is provided, and the heavy materials handling operation is completed while the robot system and the environment are not damaged.

The power assist ratio (λ), suggested in (1) and (2), plays a role of controlling the scale of the force that is required by an operator for a human-robot cooperation-work. In the experiments, we studied changes of F_h and F_e when the power assist ratio (λ) was increased from 3 to 6. The impedance parameters for the experiments were set as $M_{pt} = 15\text{I}$, $B_{pt} = 7500\text{I}$, $M_{pe} = 50\text{I}$, $B_{pe} = 10000\text{I}$, and $K_{pe} = 8000\text{I}$. Figures 19 and 20 show the graphs of F_h and F_e, used to obtain the graph in Fig. 18.

As shown in Fig. 19 ($\lambda = 3$), F_h, for handling the object, is required to be around 10 N in case of no contact with the environment, while F_h is required to be 30 N in case of contact with the environment. As λ increased to 6 from 3, F_h, required in case of no contact with the environment, was

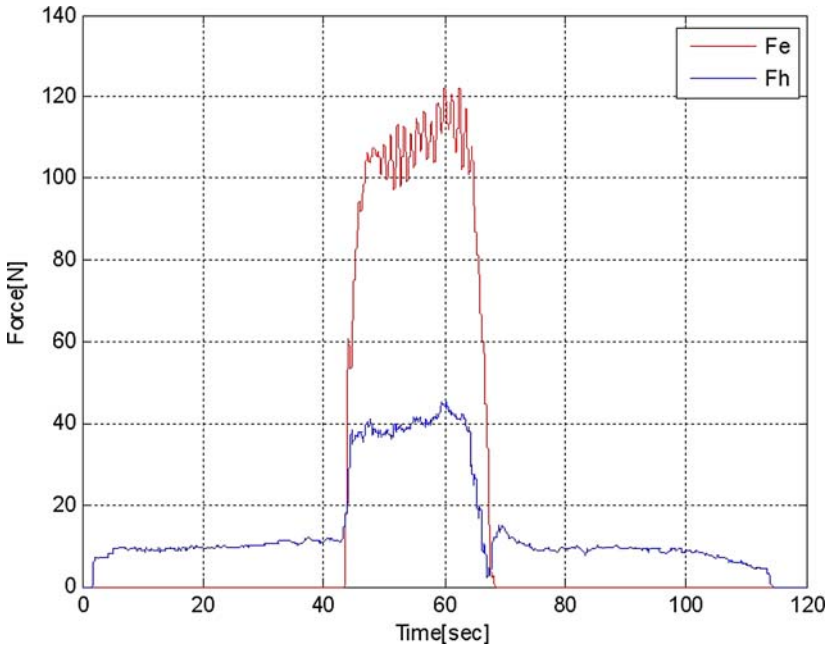

Fig. 21 F_e, F_h at $K_{pe} = 11000\text{I}$ and $\lambda = 3$

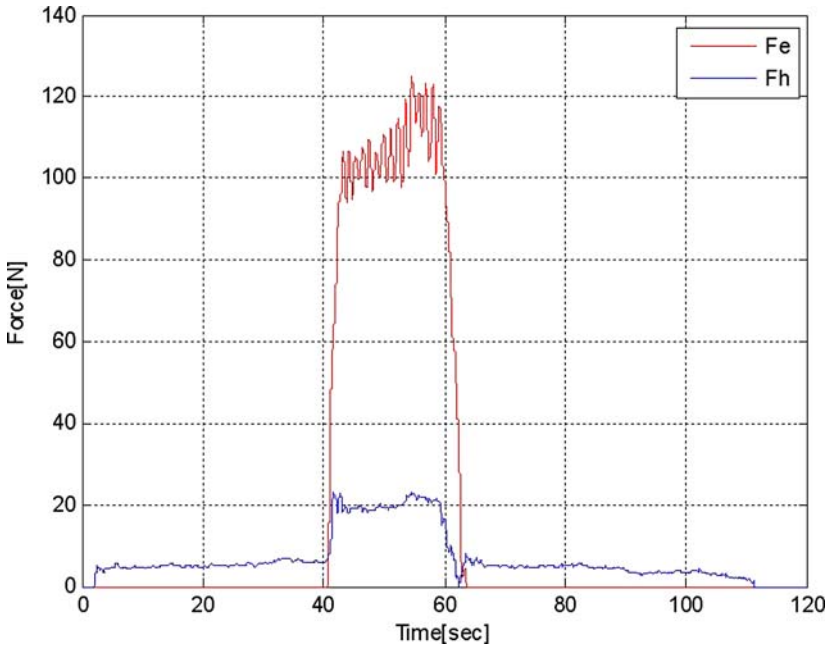

Fig. 22 F_e, F_h at $K_{pe} = 11000\text{I}$ and $\lambda = 6$

reduced by a half, and F_h for the environment-contacting case was also reduced to 15 N by around a half.

We can see that the force, required by an operator, gets smaller as λ increases, but there is no significant change in the force (F_e) that reflects in the contacting condition.

5.4 Influence of environmental stiffness parameters

The environmental stiffness (K_E) depends on the characteristics of materials, composing an environment. The purpose of this experiment, changing the environmental stiffness, lies on comparison of the reaction force (F_e) that is felt by an operator according to operational conditions such as a case contact with an obstacle occurs or a case the press fit is required. The impedance parameters for the experiment were set as $M_{pt} = 15\text{I}$, $B_{pt} = 7500\text{I}$, $M_{pe} = 50\text{I}$, $B_{pe} = 10000\text{I}$, and, $K_{pe} = 8000\text{I}$. Figures 21 and 22 show the graphs of F_h and F_e, used to obtain the graph in Fig. 18.

As shown in Fig. 21 ($K_{pe} = 11000\text{I}$), F_h of around 10 N is required to move the object in case there is no contact with the environment. In case there is contact, however, F_h (required) is around 40 N and F_E (generated) is around 100 N.

We could find that there was no change in F_h, for handling the object, in case of no contact with the environment, while F_h and F_E, for moving the object, increased from 30 N to 40 N and from 80 N to 110 N respectively in case of contact with the environment, when $K_{pe} = 8000$I (Fig. 19).

A similar result is shown when λ increases from 3 to 6 (Fig. 22). In case there is no contact with the environment, F_h of around 5 N is required to move the object. In case there is contact, however, the required force F_h is around 20 N and the generated force F_E is around 110 N. We could find that there was no change in F_h, for handling the object, in case of no contact with the environment, while F_h and F_E, for moving the object, increased from 15 N to 20 N and from 80 N to 110 N respectively in case of contact with the environment, when $K_{pe} = 8000$I (Fig. 20).

It can be recognized that, as K_{pe} increases, the force, required by an operator, gets increased and the force (F_e), reflecting in the contact condition, gets increased, too.

6 Conclusions

In this paper, we suggested a model of the human-robot cooperation system according to the contact conditions, using the adjustable impedance factors. Also, we structured the whole human-robot cooperative control system by separating into the human impedance control and the experimental impedance control with an inner motion control loop. The experimental contents can be categorized into four areas. We investigated the influences to the system of changes in the impedance parameters (M_{pt}, B_{pt}), power assist ratio (λ), and environmental stiffness parameter (K_{pe}). The influence of the inner motion control loop against the system was also studied. The experimental results showed that the force, required by an operator, got decreased as λ increased, but there was no change in the force (F_e), reflecting in the contact condition. On the contrary, as K_{pe} increased, the force, required to an operator, increased, and the force (F_e), reflecting in the contact condition, also increased. Through the experiments, we could observe the characteristics of the power assist and the force reflection, the merits of the human-robot cooperation system.

If we properly apply the human-robot cooperative control system, mentioned in this paper, to heavy-materials handling works at construction sites, operators can move heavy materials with relatively less force, while complying with the operators' intention. Also, it allows operators to promptly respond to work environments, changing in real time, through the intuitive force reflection in the environmental-contacting conditions especially during operations such as combining heavy material together or press fit work.

In near future, a construction robot for installation of heavy construction materials, to which the suggested human-robot cooperative control system is to be applied, will be developed.

Acknowledgment This work was supported by the SAMSUNG CORPORATION and the SRC/ERC program of MOST (grant#R11-2005-056-03003-0).

References

Choi, H.S., Han, C.S., Lee, K.Y., and Lee, S.H. 2005. Development of hybrid robot for construction works with pneumatic actuator. *Automation in Construction*, 14(4):452–459.

Fukuda, T., Fujisawa, Y., et al. 1991a. A new robotic manipulator in construction based on man-robot cooperation work. In *Proc. of the 8th International Symposium on Automation and Robotics in Construction*., pp. 239–245.

Fukuda, T., Fujisawa, Y., Kosuge, K., et al 1991b. Manipulator for Man-Robot Cooperation. *International Conference on Industrial Electronics, Control and Instrumentation*, 2:996–1001.

Fukuda, T., Fujisawa, Y., Arai, F., et al. 1991c. Study on man-robot cooperation work-type of manipulator. 1st Report, Mechanism and Control of Man-Robot Cooperation Manipulator, Trans. Of the JSME, pp. 160–168

Gambao, E., Balaguer, C., and Gebhart, F. 2000. Robot assembly system for computer-integrated construction. *Automation in Construction*, 9(5/6):479–487.

Hogan, N. 1985. Impedance control: An approach to manipulation, Part I-III. *ASME Journal of Dynamic Systems, Measurements and Control*, 107:1–24.

Isao S., Hidetoshi O., Nobuhiro T., and Hideo T. 1996. Development of automated exterior curtain wall installation system. International Symposium on Automation and Robotics in Construction (ISARC'96), Tokyo, Japan.

Kazerooni, H. 1989. Human/robot interaction via the transfer of power and information signals – part I: Dynamics and control analysis. In *IEEE Proc. of IEEE International Conference on Robotics and Automation*, pp. 1632–1640.

Kazerooni, H. 1989. Human/robot interaction via the transfer of power and information signals – part II: An experimental analysis. In *IEEE Proc. of IEEE International Conference on Robotics and Automation*, pp. 1641–1647.

Kazerooni, H. and Mahoney, S.L. 1991. Dynamics and control of robotic systems worn by humans. *ASME Journal of Dynamic Systems, Measurement and Control*, 133(3):379–387

Kosuge K., Fujisawa, Y., and Fukuda, T. 1993. Mechanical system control with man-machine-environment interactions. In *Proc. of IEEE International Conference on Robotics and Automation*, pp. 239–244.

Lee, S.Y., Lee, K.Y., Park, B.S., and Han, C.S. 2006. A Multidegree-of-freedom manipulator for curtain-wall installation. *Journal of Field Robotics*, 23(5):347–360.

Masatoshi, H., Yukio, H., Hisashi, M., Kinya, T., Sigeyuki, K., Kohtarou, M., Tomoyuki, T., and Takumi, O. 1996. Development of interior finishing unit assembly system with robot: WASCOR IV research project report. *Automation in Construction*, 5(1):31–38.

Miller, J.S. 1968. The Myotron—A Servo-controlled exoskeleton for the measurement of muscular kinetics. Cornell Aeronautical Laboratory Report VO-2401-E-1.

Mosher, R.S. 1967. Handyman to Hardiman. Automotive Engineering Congress. SME670088

Ostoja-Starzewski, M. and Skibniewski, M. 1989. A master-slave manipulator for excavation and construction tasks. *Robotics and Autonomous Systems*, 4(4):333–337.

Roozbeh, K. 1985. Advanced robotics in civil engineering and construction. In *International Conference on Advanced Robotics (ICRA '85)*, St. Louis, Missouri.
Santos, P.G., Estremera, J., Jimenez, M.A., Garcia, E., and Armada, M. 2003. Manipulators helps out with plaster panels in construction. *The Industrial Robot*, 30(6):508–514.
Skibniewski, M.J. 1988. *Robotics in Civil Engineering*. Van Nostrand Reinhold, New York.
Skibniewski, M.J. and Wooldridge, S.C. 1992. Robotic materials handling for automated building construction technology. *Automation in Construction*, 1(3):251–266.
Warszawski, A. 1985. Economic implications of robotics in building. *Building and Environment*, 20(2):73–81.

Seung Yeol Lee received the B.S. degree from the Department of Mechanical Engineering, Myungji University, Seoul, Korea in 2002, and the M.S. degree from the Department of Mechatronics Engineering, Hanyang University, Seoul, Korea in 2005. He is a Ph.D. degree candidate from the Department of Mechanical Engineering, Hanyang University, Seoul, Korea. From 2003, He is currently a visiting researcher in the Research Institute of Technology, Construction Group at the Samsung Corporation, Korea conducting the design and implementation of construction robot and automation system for construction project. His research interests include design, control, and application of construction robots, field robotic systems and ergonomic design of robotic systems. He is a member of the Korea Society of Mechanical Engineers, Architectural Institute of Korea, and Ergonomics Society of Korea.

Kye Young Lee received the B.S degree in mechanical engineering in 1996 from Hanyang University, Ansan, Korea, and both the M.S degree in precision mechanical engineering and Ph.D. degree in mechanical engineering from Hanyang University, Seoul, Korea, in 1998 and 2006, respectively.
From 2001, He is currently a research engineer in the Research Institute of Technology, Construction Group at the Samsung Corporation, Korea conducting the design and implementation of construction robot and automation system for construction project.
His research interests include human-robot cooperative works, human-robot interactive system, embedded system control in robotics, application of field robot, and application of robotic system in construction industry.

Sang Heon Lee graduated with the B.S. degree in Precision Mechanical Engineering from Hanyang University, Seoul, Korea in 1992. He received the M.S. degree in Precision Engineering from KAIST, Taejon, Korea in 1994 and the Ph.D. degree in Mechanical Engineering from KAIST in 2001. Currently, he is a senior researcher in Samsung Corporation, Korea. His major interests include the kinematic/dynamic analysis on multi-body system, application of field robots, and automation in construction.

Jin Woo Kim received the B.S. degree from the Department of Mechanical Engineering, Hanyang University, Seoul, Korea in 1996, and the M.S. degree from the Department of Mechatronics Engineering, Hanyang University, Ansan, Korea in 1999. He is a Ph.D. degree candidate from the Department of Mechatronics Engineering, Hanyang University, Ansan, Korea. He is a member of the Korea Society of Mechanical Engineers, Architectural Institute of Korea. His research interests include kinematic analysis, design of pantograph systems and application of robotic systems. Since 2005, He is currently as a research engineer in the High-Speed Rail Division, at the Korea Railroad Research Institute.

Chang Soo Han received the B.S. degree from the Depart ment of Mechanical Engineering, Seoul National University Technology, Seoul, Korea in 1983, and the M.S. and Ph.D. degrees from the Department of Mechanical Engineering, University of Texas at Austin, in 1985 and 1989, respectively. From May 1988 to September 1989, he was a Research Assistant, Robotics Lab in Mechanical Engineering about manufacturing of the high resolution micro manipulator module. In March 1990, he joined Hanyang University, Ansan, Kyungki-Do, Korea as a Professor, Department of Mechanical Engineering. From March 1993 to February 1995, he was a Vice President, The Research Institute of Engineering & Technology of the Hanyang University. From August 1996 to July 1997, he was a Visiting Professor, Univ. of California at Berkeley. From September 1997 to February 1999, he was a Director, Hanyang Business Incubator. In August 2000, he joined a Branch

President, The Korean Society of Mechanical Engineers. In January 2002, he joined a Committee Member, The Korean Society of Mechanical Engineers. From January 2001 to December 2001, he was an International Cooperation Director, The Institute of Control, Automation and Systems, Korea. His research interests include design, control, and application of robot, automation systems, and advanced vehicle.